
# Fibre Optic Nonlinear Technologies [FONTE] - A European Industrial Doctorate [GA766115]

## Document Details

| | |
|---|---|
| Title | Deliverable 5.3 Quantification of performance degradation due to components imperfection |
| Deliverable number | D5.3 |
| Deliverable Type | Report (public) |
| Deliverable title | Quantification of performance degradation due to components imperfection |
| Work Package | WP5 – Experimental implementation and testing of NFT systems (RO4 RO5, TO1, TO2) |
| Description | |
| Deliverable due date | 31/01/2021 |
| Actual date of submission | 29/09/2021 |
| Lead beneficiary | 2 - ALUD |
| Version number | V1.1 |
| Status | FINAL |

## Dissemination level

| | | |
|---|---|---|
| PU | Public | X |
| CO | Confidential, only for members of the consortium (including Commission Services | |

## Project Details

| | |
|---|---|
| Grant Agreement | 766115 |
| Project Acronym | FONTE |
| Project Title | Fibre Optic Nonlinear Technologies |
| Call Identifier | H2020-MSCA-ITN-2017 |
| Project Website | fonte.astonphotonics.uk |
| Start of the Project | 1 June 2018 |
| Project Duration | 48 months |

## Consortium

Aston University

NOKIA Bell Labs

TELECOM ParisTech

TU Delft

DTU Technical University of Denmark

## EC Funding

This project has received funding from the European Union's Horizon 2020 research and innovation programme under the Marie Skłodowska-Curie grant agreement No 766115

# Executive Summary

ESR1 presents a new design of a neural-network-based signal equalizer of channel and transceiver device distortions. The performance gains of the proposed equalizer were investigated numerically in several metro fiber systems and experimentally in at 612 km G.652 SSMF field trial. Moreover, for every studied testcase a Bayesian optimizer was used to fine-tune the hyper-parameters of the proposed architecture. The presented numerical and experimental results demonstrate that the proposed NN leads to significant system performance improvement, which originates not only from the fiber nonlinearity mitigation but also from the transceiver device distortion compensation.

ESR2 reviewed the undesired responses of a typical coherent optical transmitter. He proposed a NN-based digital pre-distortion (DPD) schemes in order to mitigate these responses at the transmitter side. The proposed technique was tested on a high symbol rate system. The scheme shows significant gains achieved by compensating the responses of transmitter components.

ESR3 presents two different reliable, low-latency receiver solutions for intensity-modulated and directed detected (IM/DD) transmission system used in low-cost short reach optical applications. In those systems, chromatic dispersion is the main limitation for higher symbol rate systems. To overcome this challenge, ESR3 have proposed a receiver consisting of optical filters that slices the signal into smaller sub-bands and each is detected by a photodetector. Then the signal reconstruction and CD compensation is studied and compared by applying different equalization: either a linear feedforward equalizer, or feedforward neural network and reservoir computing. The performance of these different receivers is compared experimentally.

ESR4 considers deep-learning based solutions to tackle the nonlinearity compensation in optical fiber communications. Several different neural network based equalization are compared in numerical simulation of single-polarization long-haul coherent transmission system. In particular, equalizers based on either feedforward neural networks (FFNN), or convolutional neural networks (CNN), recurrent neural networks (RNN) are optimized and their performance is compared for different link lengths.

# TABLE OF CONTENTS

# LIST OF FIGURES



# LIST OF ACRONYMS

| | |
|---|---|
| AiPT | Aston Institute Of Photonic Technologies |
| AWGN | Additive White Gaussian Noise |
| BPD | Balanced Photo-Diodes |
| BER | Bit Error Rate |
| CD | Chromatic Dispersion |
| CDC | Chromatic Dispersion Compensation |
| CNN | Convolutional Neural Network |
| DA | Driver Amplifier |
| DAC | Digital to Analog Converter |
| DPD | Digital Pre-Distortion |
| DSP | Digital Signal Processing |
| DWDM | Dense Wavelength Division Multiplexing |
| EC | European Commission |
| EID | European Industrial Doctorates |
| ESR | Early Stage Researcher |
| ECL | External Cavity Laser |
| EDFA | Erbium-Doped Fiber Amplifier |
| FFE | Feed Forward Equalizer |
| FFNN | Feed Forward Neural Network |

| | |
|---|---|
| FONTE | Fibre Optic Nonlinear Technologies |
| HWHM | Half-Width Half-Maximum |
| IM/DD | Intensity Modulated Direct Detection |
| LEAF | Large Effective Area Fiber |
| LO | Local Oscillator |
| MZM | Mach-Zehnder Modulator |
| NN | Neural Network |
| OOK | On-Off Keying |
| PME | Polarization Multiplexing Emulator |
| QAM | Quadrature Amplitude Modulation |
| RC | Reservoir Computing |
| RNN | Recurrent Neural Network |
| RRC | Root-raised Cosine |
| RTO | Real Time Oscilloscope |
| SCM | Subcarrier Multiplexing |
| SMF | Single Mode Fiber |
| SNR | Signal to Noise power Ratio |
| sps | samples per symbol |
| SSMF | Standard Single-Mode Fiber |
| WDM | Wavelength-Division Multiplexing |
| WSS | Wavelength Selective Switch |

# 1 RECEIVER-BASED ESTIMATION AND COMPENSATION OF TRANSCEIVER NONLINEARITIES

During his work, ESR1 contributed to a technique of the receiver-based transceiver nonlinearities compensation. Particularly, a novel design of a complex-valued neural network was developed for the signal equalization on the receiver side. The results of this work were published in [1] which are briefly explained in this deliverable. For detailed explanation, interested readers are referred to [1]. The design was made under the assumption of Kerr nonlinearity being the leading distortion in the link, however, in the presence of considerable device impairments. The performance of the proposed architecture was investigated both numerically and experimentally for application on metro networks with either standard single-mode fiber (SSMF) and large effective area fiber (LEAF). The proposed solution was compared with the dense neural network proposed in [2] and the standard digital back-propagation [3]. Moreover, the Bayesian optimizer was implemented to fine-tune the hyper-parameters of the proposed architecture for every considered testcase.

Let's briefly describe the proposed architecture. The pass-averaged Manakov equations [4] describes the averaged evolution of the slowly-varying complex-valued envelopes of the electric field in an optical fiber

$$\frac{\partial u_{H/V}}{\partial z} = \frac{G(z)}{2} u_{H/V} - i\frac{\beta_2(z)}{2}\frac{\partial^2 u_{H/V}}{\partial t^2} + i\frac{8\gamma(z)}{9}(|u_H|^2+|u_V|^2)u_{H/V} + \xi(z,t). \quad (1.1)$$

Here $u_{H/V}(t,z)$ are the normalized optical fields of horizontal (*H*) and vertical (*V*) polarization, respectively, $\beta_2$ is the group velocity dispersion, $\tilde{\gamma} = \gamma e^{-\alpha z}$ is the effective averaged nonlinearity coefficient, that includes the effective length scale $L_{eff} = (1 - e^{-\alpha L})/\alpha$ emerging due to averaging over periodic loss and gain, $\gamma$ is the fiber nonlinear coefficient, $L$ is the span length and $\alpha$ is the fiber loss coefficient. For the memoryless case $\beta_2 = 0$, one can express the analytical solution of Eq. (1.1) assumed by the H-polarization of signal $u_{H/V}(t,z)$ at the end of the transmission link [5]

$$x_{H_k} = y_{H_k} e^{-j\gamma L_{eff}\frac{8}{9}N_s\left[|y_{H_k}|^2+|y_{V_k}|^2\right]}. \quad (1.2)$$

Here $X_{Hk}$ and $Y_{Hk}$ are the transmitted and received soft symbols.

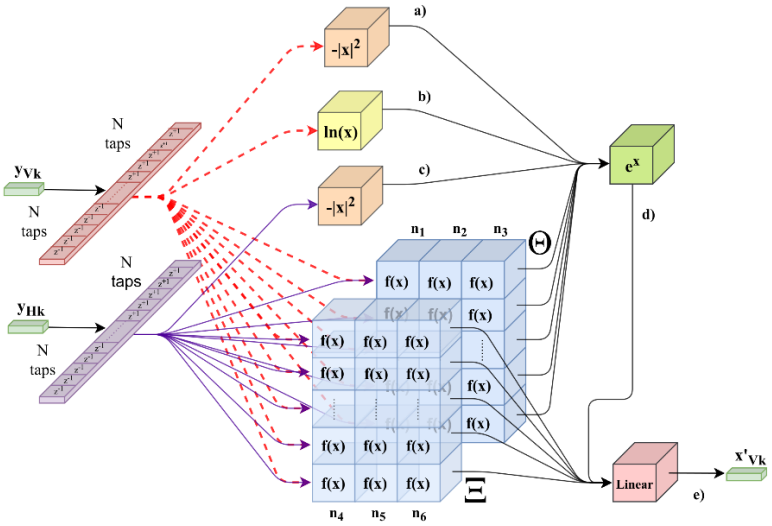


*Figure 1.1: The architecture of the proposed NN.*

Based on Eq. (1.2) and the previously suggested high-nonlinearity approximations for the optical channel [6], the neural network (NN) architecture was proposed as shown Figure 1.1: The architecture of the proposed NN. Here $Y_{V/H_k}$ is the sequence of received symbols $\left[y_{V/H_{k-N}}, \dots, y_{V/H_k}, \dots, y_{V/H_{k+N}}\right]$, $x'_{V/H_k}$ is the prediction for the $k$-th symbol in the polarization of interest, $2N+1$ is the model memory size, and $\Theta, \Xi$ are three-layer dense neural networks approximating the nonlinear functions covering the gaps between the idealistic model Eq. (1.2) and the real-world link. To process properly the complex-values, the proposed NN utilized the following custom complex-valued activation function

$$f(x = x_r + jx_i) = \frac{e^{2x_r} - 1}{e^{2x_r} + 1} + j\frac{e^{2x_i} - 1}{e^{2x_i} + 1}. \quad (1.3)$$

The hyper-parameters of the model: half-memory size $N$, and the sizes of each of $\Theta, \Xi$ layers, were learnt for every considered testcase via hyper-parameter optimization [7] with the found parameters given in [1].

## 1.1 Obtained Results

The numerical and experimental tests of the proposed NN were conducted. During numerical simulations we considered 6x80 km and 12×80 km systems built out of LEAF ($\alpha = 0.225$ dB/km, $\beta_2 = 4.2$ ps/(nm*km), $\gamma = 1.3$ (W*km)$^{-1}$) or SSMF ($\alpha = 0.21$ dB/km, $\beta_2 = 16.8$ ps/(nm*km), $\gamma = 1.14$ (W*km)$^{-1}$) spans. Each span in numerical system was followed by an EDFA with noise figure 5 dB. The scheme of the numerically tested system is given in Figure 1.2:The experimentally measured performance of the proposed NN. We compared the NN with the conventional DSP, represented in the simulations by the chromatic dispersion compensation (CDC), followed by an amplitude-phase shift of the received signal to the transmitted one. The application of the proposed NN resulted in the following gains: 2.16 dB for LEAF 6x80km, 1.25 dB for LEAF 12x80km, 0.36 dB for SSMF 6x80 km, 0.38 dB for SSMF 12x80km. Moreover, the optimal launch power is increased for the proposed NN in all the numerically considered testcases. This shows that SNR gains were obtained mostly by the nonlinearity compensation.

In the experimental study, the same field trail setup as in [9] was used to collect the data. The link was formed by 8×78 km G.652 SSMF spans and the two 2 km long SSMF connectors, having the total length 612 km. The link is deployed between Torino and Chivasso in Italy. The transmitted spectrum was formed by a 200G channel under test surrounded by 15×200G dummy 16QAM channels to the left- and right-hand sides, leading to a 31 channel WDM transmission in the 37.5 GHz grid (33 GBaud). At the receiver side, the channel of interest was filtered out of the received signal, received by a coherent receiver and processed by a conventional digital signal processing (DSP) [10].

Figure 1.2:The experimentally measured performance of the proposed NN. illustrates the obtained experimental results. The proposed NN is compared there with the raw data after DSP (marked as CDC+norm in the figure legend) and the published NLC DNN [2]. First, the proposed NN caused a 2 dB SNR gain and a 2 dB increase in optimal launch power when compared with the raw DSP data. Second, unlike the numerical results, in the experiment the proposed NN led to ≈1.6 dB SNR gain at lower powers in the linear regime. This result indicates that the proposed NN is able to mitigate the impact of not only the channel nonlinearity, but also device impairments such as, e.g., the impact of low-resolution digital-to-analog converters, the driver amplifier, and the dual polarization Mach-Zehnder modulator imperfections.

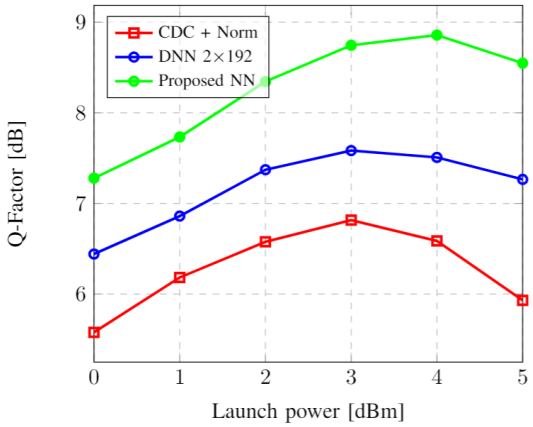


*Figure 1.2:The experimentally measured performance of the proposed NN.*

## 1.2 REFERENCES (THIS SECTION)

[1] Freire, P.J., Neskorniuk, V., Napoli, A., Spinnler, B., Costa, N., Khanna, G., Riccardi, E., Prilepsky, J.E. and Turitsyn, S.K., 2020. Complex-Valued Neural Network Design for Mitigation of Signal Distortions in Optical Links. *Journal of Lightwave Technology*.

[2] O. S. Sidelnikov, A. A. Redyuk, S. Sygletos, and M. P. Fedoruk, "Methods for compensation of nonlinear effects in multichannel data transfer systems based on dynamic neural networks," *Quantum Electronics* 49, p. 1154, (2019).

[3] E. Ip, and J.M. Kahn "Compensation of dispersion and nonlinear impairments using digital backpropagation," *Journal of Lightwave Technology* 26, p. 1154, (2008).

[4] R.-J. Essiambre, G. Kramer, P. J. Winzer, G. J. Foschini, and B. Goebel, "Capacity limits of optical fiber networks," *Journal of Lightwave Technology* 28, 662–701 (2010).

[5] G. P. Agrawal, "Nonlinear science at the dawn of the 21st century," Lecture Notes in Physics, vol. 542, pp. 195–211, 2000.

[6] V. Oliari, E. Agrell, and A. Alvarado, "Regular perturbation on the group-velocity dispersion parameter for nonlinear fibre-optical communications," *Nature communications* 11, pp. 1–11, 2020.

[7] M. Pelikan, D. E. Goldberg, E. Canť u-Paz et al., "Boa:The bayesian optimization algorithm," in *Proceedings of the genetic and evolutionary computation conference (GECCO-99)*, vol. 1, 1999, pp. 525–532, 1999.

[8] G. P. Agrawal, "Nonlinear fiber optics," pp. 195–211, 2000.

[9] G. Khanna, T. Rahman, E. De Man, E. Riccardi, A. Pagano, A. C. Piat, B. Spinnler, S. Calabro, D. Rafique, U. Feiste et al., "Comparison of single-carrier 200G 4QAM, 8QAM and 16QAM in a WDM field trial demonstration over 612 km SSMF," in *42nd European Conference on Optical Communication (ECOC 2016)*, pp. 1–3, 2016.

[10] M. S. Faruk, S. J. Savory, "Digital signal processing for coherent transceivers employing multilevel formats". *Journal of Lightwave Technology*. 2017 Mar 1;35(5):1125-41.

# 2 NEURAL NETWORK-BASED DIGITAL PRE-DISTORTION OF COHERENT OPTICAL TRANSMITTER

A typical fiber-optic transmission system suffers from the distortions generating from the undesired responses of its transceiver components. In the next generation transceivers, which are being designed to modulate higher order formats such as 64-QAM, compensation of the responses from the imperfect components becomes crucial in order to achieve the maximum information transmission rate. ESR2 has been working on identification of transmitter impairments in high symbol-rate transceivers and has been studied design of efficient nonlinear digital pre-distortion based on neural networks to pre-compensate those impairments.

## 2.1 COHERENT OPTICAL TRANSMITTER

In a typical coherent optical transmitter, each of its key blocks have undesired responses. In the following each key block of transmitter is reviewed with focus on their transfer responses.

### 2.1.1 Digital To Analog Converter (DAC)

A DAC generates a continuous-time waveform from a given sequence of data samples. The complex signal is produced as two tributaries namely in-phase "I" and quadrature phase "Q". Typically, DACs have limited physical number of bits to generate a waveform. The incoming data sequence is first quantized to a limited number of quantization levels of the DAC, as shown in Figure 2.1(a), causing a nonlinear distortions in the signal, usually termed as quantization noise. In addition, the DACs have limited electrical bandwidth because of which the output voltage of the DAC reduces significantly at higher frequencies. As shown for example in Figure 2.1(b), the DAC has around 24 GHz of 3-dB bandwidth. In absence of pre-emphasis the higher frequency components will be significantly attenuated at the DAC output.

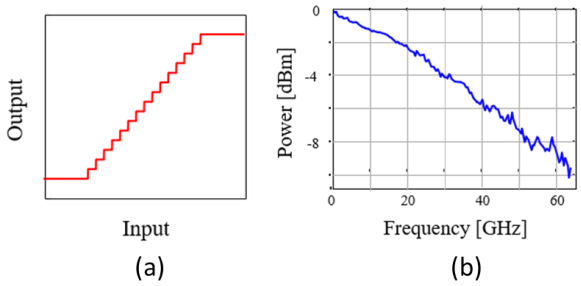


*Figure 2.1: Response of a DAC (a) Nonliear resonse due to quantization, (b) Limited electrical bandwidth.*

### 2.1.2 Driver Amplifier (DA)

Driver amplifiers are needed to raise the power of the DAC output waveform to sufficiently high in order to drive the optical modulator. DAs also have nonlinear behaviour caused by gain compression as shown in Figure 2.2(a). A standard formula to model the nonlinear behaviour of a DA is given by [1]

$$V_{out} = \frac{gV_{in}}{\left(1 + \left(\frac{g|V_{in}|}{V_{sat}}\right)^{2p}\right)^{1/2p}}$$

where $V_{in}$, $V_{out}$ and $V_{sat}$ are the input, output and saturation voltages of the DA, while g is the small signal gain. The typical value of the nonlinearity parameter p is 2. In addition to gain-compression the transfer characteristic of DA is often asymmetric with respect to the polarity of the signal. This, for an example, causes

more compression of the signal in the negative voltage range. The electrical bandwidth of the DA is also limited. An example of the linear response of a DA with 46 GHz bandwidth is shown in Figure 2.2(b).

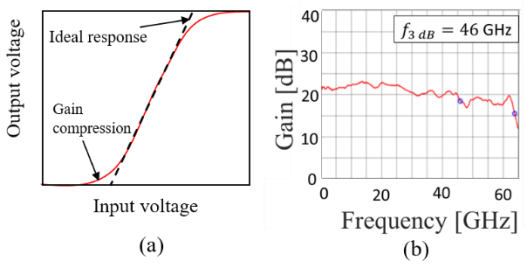


*Figure 2.2: Response of a driver amplifier (a) Nonlinear gain, (b) Limited electical bandwidth.*

### 2.1.3 Optical Modulator

In high-speed optical transmitters, the signal is modulated by an optical carrier using the external modulator like Mach-Zehnder modulator (MZM). In fact, a complex-valued signal is produced by using two separate MZ interferometer structure for modulation of the I and the Q tributaries, often called as IQ modulator. The modulator inherently has a sinusoidal response, which comes from its working principle. In addition to the inherent sinusoidal characteristic, there is non-ideal characteristic due to the manufacturing defects such as gain imbalance between two arms. These effects in altogether contribute to the distortions in the modulated optical signal. The sinusoidal response of MZ structure (shown in Figure 2.3(a)) can be modelled by the following equation [2]

$$E_{out} = \frac{1}{2}\left(e^{\frac{j\pi V_{in}}{2V_\pi}} + j\,\gamma\, e^{-\frac{j\pi V_{in}}{2V_\pi} + j\phi}\right)$$

where $V_{in}$=1 is the input (I/Q) signal to the modulator and $V_\pi$ is the voltage required for inducing a phase change of $\pi$ radians. The gain and phase imperfection of the modulator can be modelled using gain-imbalance $\gamma$ and phase imperfection $\phi$ parameter. The electro-optical bandwidth of the modulator is also limited as shown in Figure 2.3(b).

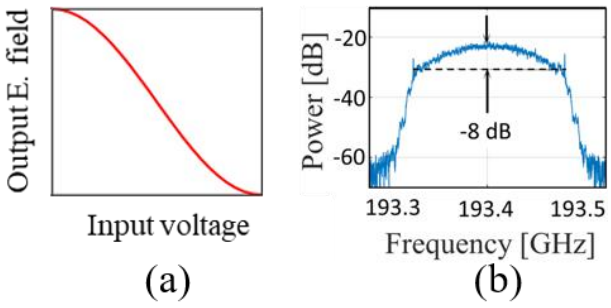


*Figure 2.3: Response of a MZM (a) Nonlinear response, (b) limited optical bandwidth.*

In addition to the distortions from the above key blocks, the transmitter typically suffers from signal-reflections that are originated by the radio frequency (RF) cables/connections. In the following, we apply transmitter-side digital pre-distortion (DPD) technique or receiver-side equalizer in order to compensate for the undesired responses discussed above.

## 2.2 TRANSMITTER DIGITAL PRE-DISTORTION

Digital Pre-Distortion (DPD) is a well-known technique to pre-compensate the undesired response of the components. In coherent optical transmitter, a DPD can be applied on the symbol sequence prior to loading it into the DACs. Usually, a linear DPD is applied at the transmitter as linear effects are more dominant and relatively less difficult to determine. A linear DPD can compensate for the limited electrical bandwidth and signal reflections, however, nonlinear effects remain uncompensated which in turn limit the power that can be applied to the transmitter components. In the fiber-optic transceiver that modulate higher order formats such as 64-quadrature amplitude modulation (64-QAM), nonlinear responses of the components can significantly degrade the signal integrity. Thus, a nonlinear DPD may require. Nonlinear DPDs improve signal integrity not only by compensating the nonlinear response of the components but also allow us to apply high power to the components.

In fiber-optic communication, many techniques were so far presented to apply nonlinear DPD such as the ones based on the Volterra-series and look-up tables. Recently, we proposed a NN-based DPD which was trained and tested on experimental setup [3]. The proposed DPD was designed using simple FFNNs and convolutional NNs. The description of the NN-based DPD is given in the following section.

### 2.2.1 NN-based Digital Pre-Distortion

The proposed architecture of the NN-based DPD is shown in Figure 2.4. Its architecture was optimized in numerical simulations by modelling a coherent optical transmitter. We used the previously discussed simulated and experimental responses of the components in order to model the transmitter. The NN was implemented using real values and hence, two separate NNs are needed to compensate for the distortions in I and Q tributaries. In the beginning, there is a uni-dimensional linear CNN with 101 taps. The output of the CNN is then fed a FFNN. The first layer in the FFNN is another 1-D linear CNNs with 11 taps feeding to 21 neurons. The following layers are fully connected layers with 12, 8 and 8 neurons with nonlinear activation function of leaky rectified linear unit (Leaky ReLU). A layer with single linear neuron follows and completes the FFNN part. Another 1-D CNN layer with 301 taps follows the FFNN. We introduce a customized activation function, which we call as “soft-DAC”. Soft-DAC unit is a piece-wise linear function models the DAC in NN and optimizes the clipping and quantization noise. Two batch normalization (BN) layers were added before and after the Soft-DAC in order to integrate our Soft-DAC implementation with the complete NN architecture.

The proposed NN-based DPD was trained using a well-known direct learning architecture (DLA). Another NN was used to serve as an auxiliary model to facilitate the training using DLA. Further details about the proposed NN-based DPD can be found in our recent paper [3].

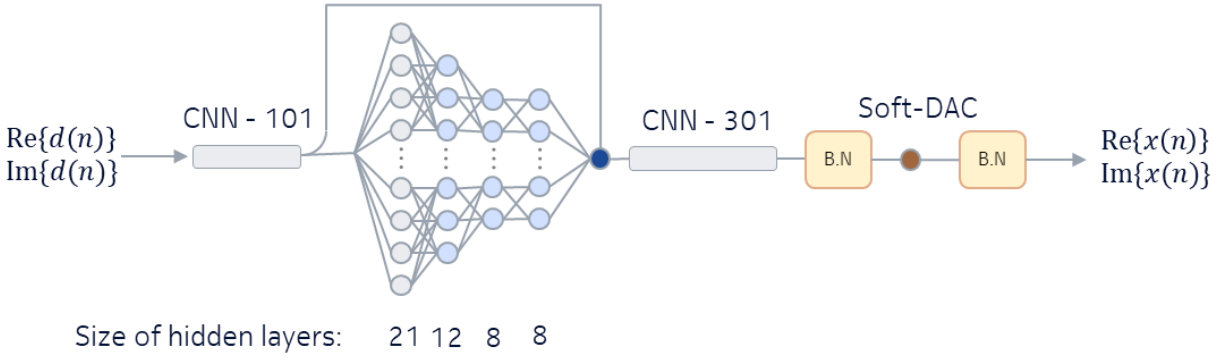


*Figure 2.4: Architecture of the proposed NN-based DPD.*

### 2.2.2 Experimental Setup

A 128 GBaud optical coherent transmission setup was considered to test our proposed DPD. A schematic of the experimental setup is shown Figure 2.5. A sequence of $2^{15}$ symbols of a probabilistic constellation shaping (PCA) 256-(quadrature amplitude modulation) QAM signal was used as data. The PCS 256-QAM symbol sequence was drawn from the Maxwell-Boltzman distribution with an entropy of 7.5 bits/symbol. At the transmitter, first DPD is applied to obtain the pre-distorted sequence, which are then loaded into the DACs' memory. The DACs have 24 GHz 3-dB bandwidth and a nominal resolution of 8 bits respectively. The DACs produce waveform at 128 GSa/s. Two driver amplifiers (DAs) which have 3-dB bandwidth of about 60 GHz amplify the DACs' output signal. A lithium-niobate ($LiNbO_3$) IQ modulator with 41 GHz 3dB-bandwidth modulates the incoming optical carrier with the signal from DAs. The optical carrier was generated using an external cavity laser (ECL) at 193.5 GHz with 20 kHz linewidth. A polarization multiplexing emulator (PME) with decorrelation delay of 54 ns was used to generate a dual polarization optical signal. An Erbium doped fiber amplifier (EDFA) boosts the power of the DP PCS-256QAM signal. The low-pass response of the IQ modulator is corrected by the Finisar Waveshaper by flattening the optical spectrum of the signal. The setup was either configured in a back-to-back or an 80 km fiber transmission scenario. In case of the back-to-back transmission signal passes through two EDFAs and reaches the receiver. At the receiver, the signal was filtered by an optical band-pass filter with 128 GHz 3-dB bandwidth. The filtered signal was then amplified by an EDFA and mixed with the local oscillator (LO) in an optical 90° hybrid. The four outputs of the hybrid are detected using four balanced photo-diodes (BPDs). The detected signals were sampled at 256 GSa/s by a Keysight real-time oscilloscope (RTO) with a nominal resolution of 10 bits. The recorded digitized signal is then processed using an offline state-of-the-art DSP, detailed in []. In the next subsection, we present the results of this experiment.

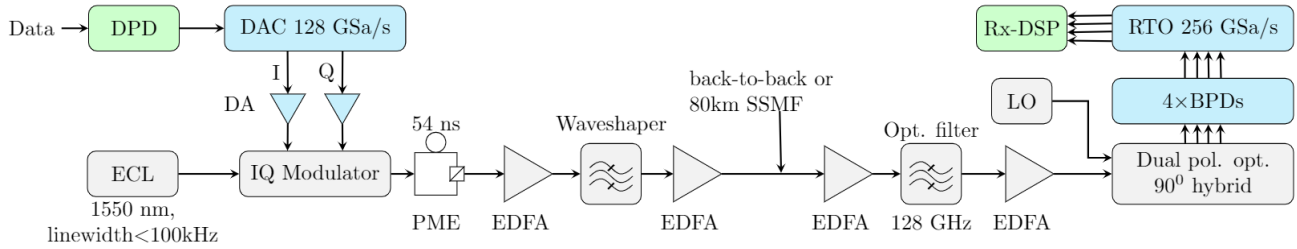


*Figure 2.5: A schematic of the 128 GBaud coherent optical transmission setup.*

## 2.3 Experimental Results

In our experiments, first, we train and test performance of both DPDs i.e. a linear DPD and NN-based DPD at different output voltages of DAC's. Figure 2.6 shows the signal-to-noise ratio of the soft symbols output from the receiver DSP. The NN-based DPD improves the SNR even for lower DACs' voltage by around 0.7 dB. With increase in DACs' voltage the SNR for the case of linear DPD decreases due to the increase nonlinear distortions. On the other hand, for the case of NN-based DPD the SNR of the received signal increases initially and reaches maximum at DACs' voltage of around 450 mV. Overall, NN-based DPD compensates for the distortions of form the transmitter components and provides a SNR gain of 1.2 dB.

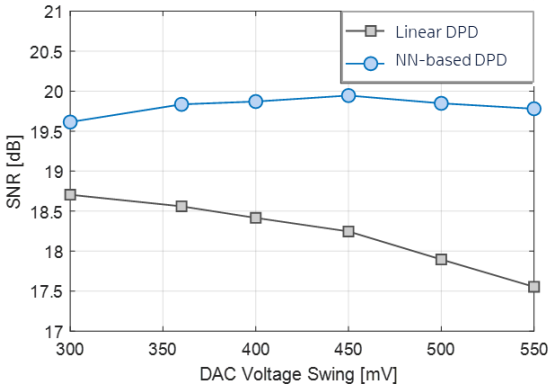


*Figure 2.6: Received SNR at different DACs' voltages.*

The effect of compensation of transmitter nonlinearity is visible in the histograms of the received signal in Figure 2.7. There is nonlinear noise (power dependent noise) present in the received signal when only a linear DPD is applied (Figure 2.7(a)). This noise is because of un-compensated nonlinear responses of the transmitter components. In Figure 2.7(b), we see by applying our proposed NN-based DPD the nonlinear noise is almost absent.

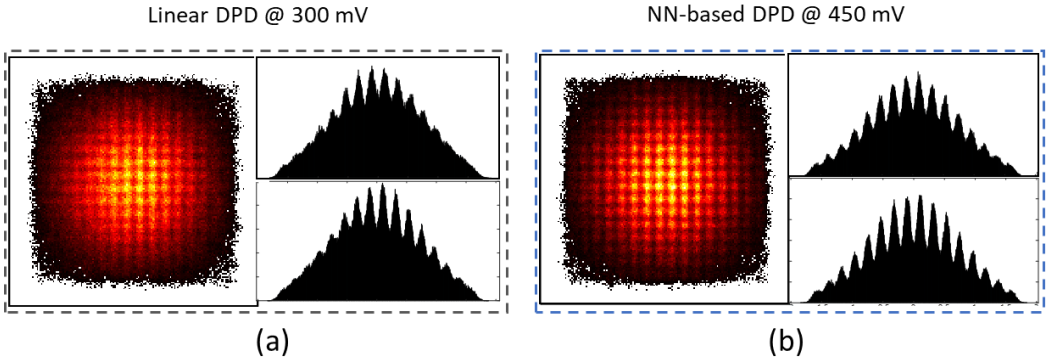


*Figure 2.7: Constellation and histograms (I and Q tributaries) of the received signal for (a) when the linear DPD is applied, (b) when NN-based DPD is applied at the transmitter.*

Next, we carried out a fiber transmission experiment. For this purpose, both DPDs were trained first in the back-to-back configuration and then were used for an 80 km standard single mode fiber transmission. We observed that NN-based DPD increases the net transmission rate from 1.51 Tb/s to a record 1.61 Tb/s over a single channel, proving its benefit.

## 2.4 Conclusion

In this deliverable, we studied NN-based digital pre-distoriton technique that is able to compensate the transmitter nonlinearity and allows achieving significant gains in the received signal SNR. The NN-based DPD increases the net transmission rate to a record 1.61 Tb/s over a single channel of 80 km optical fiber.

## 2.5 REFERENCES (THIS SECTION)

[1] C. Rapp, “Effects of HPA nonlinearity on a 4-DPSK/OFDM signal for a digital sound broadcasting signal”, ESASP, vol. 332, pp. 179--184, 1991.

[2] S. Walkin, and J. Conradi, “Effect of Mach-Zehnder modulator DC extinction ratio on residual chirp-induced dispersion in 10-Gb/s binary and AM-PSK duobinary lightwave systems”, IEEE Photonics Technology Letters, vol 9, no. 10, pp. 1400--1402, 1997.

[3] V. Bajaj, F. Buchali, M. Chagnon, S. Wahls, and V. Aref, “Single-channel 1.61 Tb/s Optical Coherent Transmission Enabled by Neural Network-Based Digital Pre-Distortion”, ECOC 2020, TuD-5.

# 3 OPTOELECTRONIC RECEIVER WITH RESERVOIR COMPUTING IN SHORT REACH OPTICAL COMMUNICATIONS

The optical communication systems are divided according to the transmission length. Considering fibers length up to ~100 km, we define the short-reach communication systems, whereas the opposite is called long-haul systems. New applications are stressing the current short-reach communication system which requires a scalably low-complexity solution to cope with this demand. One example is the upcoming 5G technology which is creating new data centers that will be located closer to the end-user, in the range of short-reach transmissions.

An attractive solution to this scenario is the use of Intensity-modulated and direct detected (IM/DD) systems which can provide low-complexity and low-latency links. However, chromatic dispersion (CD) is a major constraint to extending the transmission reach – especially for higher data-rate systems. As a solution to this impairment, ESR3 has been working on the use of hybrid optoelectronic systems, which leverage sharing the complexity between optical and electrical domains. Specifically, the proposed solution uses an optical filter and a machine-learning algorithm to mitigate the CD. The machine-learning algorithm in this case is called reservoir computing, which provides a strong advantage in the training process for nonlinear dynamic systems. Alternatively to the proposed solution, the subcarrier multiplexing (SCM) system can also be used to tackle the same problem. In this case, instead of slicing the signal before detecting – as we have proposed – the signal is already transmitted with multiple subbands in a lower symbol rate, covering the same total bandwidth as the single carrier scenario. One key difference is that the SCM system is transmitting different information in each subband, while the proposed method slices the information in the spectrum domain.

In the next section, we will compare the proposed optoelectronic system with the subcarrier multiplexing system. We show that the optoelectronic system has a 40 km increase distance compared to the proposed optoelectronic system. The results were published in [1].

## 3.1 NUMERICAL SETUP

Figure 3.1: Numerical setup describes the simulation setup used to compare the proposed optoelectronic system with the SCM. The numerical setup is divided into 2 sections to facilitate comprehension.

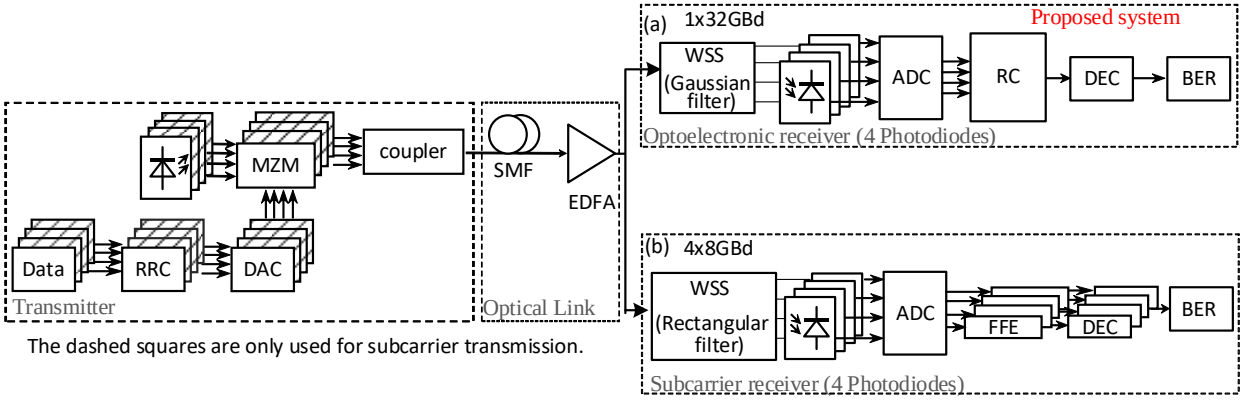


*Figure 3.1: Numerical setup (a) Single photodetector receiver. (b) Optoelectronic receiver (4 photodetector).*

## 3.2 SINGLE CARRIER TRANSMISSION

At the transmitter, a random stream of $2^{18}$ bits is generated and pulse shaped with root-raised cosine (RRC) (roll-off equal to 0.1) at 2 samples per symbol (sps), yielding a 32-GBd OOK signal. The signal is then upsampled to 8 sps and modulated by the MZM's transfer function in the quadrature point. The signal is then injected into the transmission channel. As the focus is on compensating for CD-induced ISI after detection, the transmission channel is modelled only as a linear lossless dispersive element with a dispersion parameter D = 16.4 ps/nm/km. An additive white Gaussian noise (AWGN) source is used to degrade the signal, e.g., simulating an optical pre-amplifier at the receiver, consistently with the experimental analysis. The signal-to-noise ratio (SNR) in the optical domain is kept fixed at 27 dB. At the receiver (Figure 3.1: Numerical setupa), all PDs are modelled as noiseless square-law elements. The wavelength selective switch (WSS) is modelled as 4 Gaussian filters with a half-width half-maximum (HWHM) of 8 GHz. The baseband central frequency of the filters is set to -12 GHz, -4 GHz, 4 GHz, 12 GHz. This means a spectrum overlap among the filter of 8 GHz. The reservoir computing is applied next to equalize the signal and regroup then to a single bandwidth back again. Finally, the average BER of each subcarrier is evaluated.

## 3.3 SUBCARRIER MULTIPLEXING TRANSMISSION

In the subcarrier system, the symbol rate is reduced to 8 GBd and the same process mentioned for the transmitter of the previous section is reproduced here, independently, for 4 subcarriers. Additionally, each subcarrier is shifted to a central baseband frequency of -13.2 GHz, -4.4 GHz, 4.4 GHz, 13.2 GHz, to avoid cross-talk among the carriers. The total bandwidth is also 35.2 GHz, as in the single-carrier case. After modulation, the signals are coupled together and transmitted to the SMF, as detailed in the previous section. AWGN source is added to keep the same SNR for each subcarrier as in the single carrier transmission system. At the receiver (Figure 3.1: Numerical setupb), the WSS is modelled as 4 rectangular filters with HWHM of 4 GHz. Therefore, avoiding cross-channel interference in the received signal. It should be noted that sharp filters are required in these analyses and they are a challenge to be obtained with the current technology. After filtering, the feedforward equalizer (FFE) is used to process each signal independently, and the average BER of each subcarrier is evaluated.

## 3.4 RESULTS AND CONCLUSION

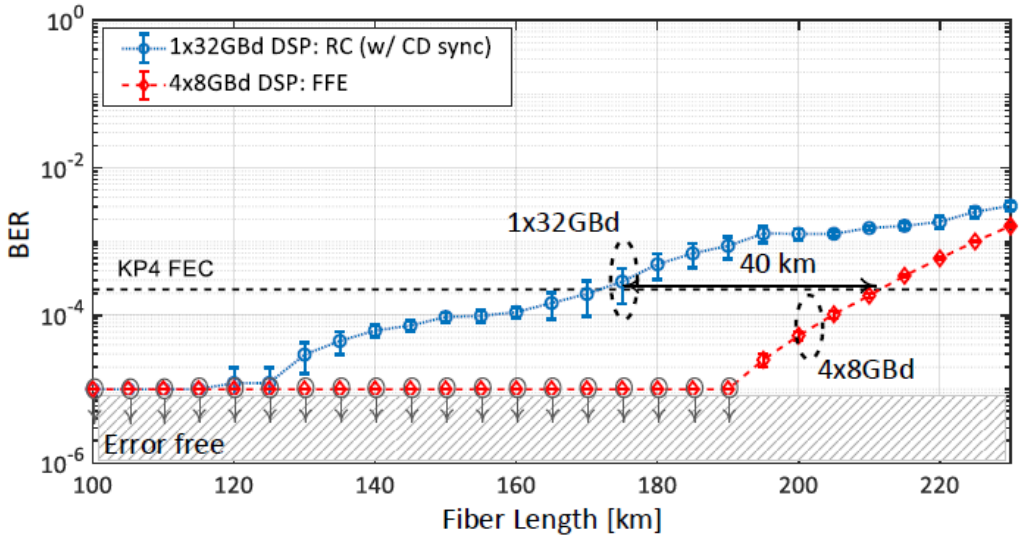


*Figure 3.2 - Numerical results comparing the proposed optoelectronic system with subcarrier multiplexed system.*

Figure 3.2 - Numerical results comparing the proposed optoelectronic system with subcarrier multiplexed system. shows the performance of a single carrier transmission for 32 GBd OOK signal using the optoelectronic receiver with 4 PDs (Figure 3.1: Numerical setupa) and the subcarrier system for 8 GBd OOK signal (Figure 3.1: Numerical setupb). The results show an improvement of 40 km in the subcarrier system receiver compared to the optoelectronic system. It is worth highlighting that the subcarrier system requires a sharp optical or digital filter in the receiver to split the subcarriers without cross-talk. A more realistic scenario would show either a penalty in spectral efficiency or performance.

## 3.5 REFERENCES (THIS SECTION)

[1] S.M. Ranzini, R. Dischler, F. Da Ros, H. Buelow, and D. Zibar," Experimental Investigation of Optoelectronic receiver with Reservoir Computing in Short Reach Optical Fiber Communications," IEEE/OSA Journal of Lightwave Technology, No. 39, 2021.

# 4 DEEP LEARNING BASED EQUALIZATION IN LONG-HAUL FIBER-OPTIC COMMUNICATIONS

ESR4 considers a deep-learning based solution to tackle the nonlinearity problem in optical fiber communications using neural network based equalizers/receivers. Signal propagation in long-haul optical fibers is subject to chromatic dispersion, Kerr nonlinearity, noise, etc. An equalizer attempts to reverse the deterministic effects of the channel by applying the inverse of the channel transformation. Digital back-propagation (DBP) based on the split-step Fourier method (SSFM) is the conventional equalization method for fiber-optic communications. But as a matter of fact, DBP suffers from a high complexity. Neural network-based equalizers are proposed as an alternative to reduce the equalization complexity while achieving the same accuracy. These models are trained using the available input-output samples of the channel by variants of stochastic gradient descent. A number of neural network models have been proposed in this regard [1].

The performance of multilayer-perceptrons (MLPs) has been discussed in several papers [2]-[4]. In [3], an MLP is used to perform equalization in a 200 Gbps DP-16QAM optical transmission system for distances 100km to 400 km. It reported a Q-factor gain of 0.5 dB to 1 dB compared to linear equalization. In [4] an MLP equalizer is used to equalize the received waveform in the nonlinear Fourier transform (NFT) domain. It is demonstrated a six-times BER improvement compared to the absence of an NN-equalizer for a 1000km optical fiber.

In [5,6], an alternative equalizer based on recurrent neural networks (RNN) is used for equalization, focusing on nonlinear and intra-channel effects mitigation. It shows that RNN based equalizers outperform the MLPs based equalizers. [7,8] has proposed a CNN based approach for the classification of different PAM classes based on the received signal as input. [9,10,11] also has proposed a CNN approach, but their model is based on the computation graph generated by SSFM. This technique termed learned DBP (LDBP), has succeeded in achieving the BER of DBP with almost 50% lower complexity.

## 4.1 SYSTEM MODEL

We considered a single-polarization optical fiber communication system where the propagation along the fiber is modelled by nonlinear Schrödinger equation

$$\frac{\partial q(t,z)}{\partial z} = -\frac{j\beta_2}{2}\frac{\partial^2 q}{\partial t^2} + j\gamma|q(t,z)|^2\, q(t,z) + n(t,z), \qquad 0 \le z \le L.$$

Where $q(t,z)$ is the complex envelope of the signal propagating in fiber as a function of time $t$ and distance $z$, $\beta_2$ is chromatic dispersion coefficient, $\gamma$ is the nonlinearity parameter, $L$ is the fiber length and $n(t,z)$ is zero-mean white circularly symmetric complex Gaussian noise with the power spectral density $\sigma_0^2$ . The fiber loss was assumed to be perfectly compensated by distributed Raman amplification.

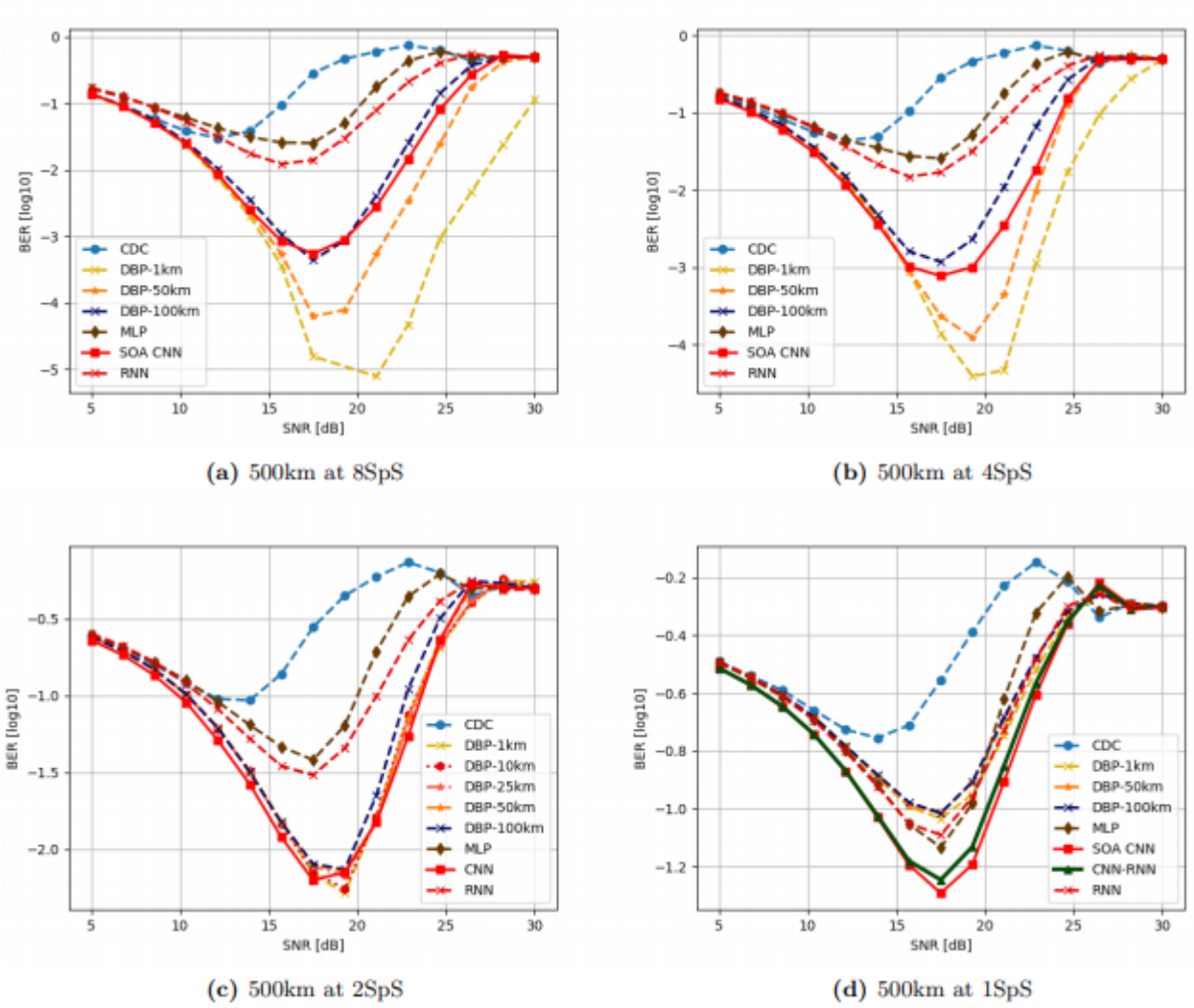


*Figure 4.1. The BER of the equalizers for the 500 km fiber-optic link, as a function of SNR for several values of sampling rates at RX and DBP step size.*

In this system, the transmitter takes a sequence of bits $\boldsymbol{m} = (m_1, \ldots, m_N)$, where $(m_{2i}, m_{2i+1}) \in \{(0,1),(1,0)\}, i = 0, \ldots, N/2$, maps it to a sequence of symbols, $\{S_i\}_{i=1}^{n}$, pulls from a quadrature amplitude (QAM) constellation, and modulates them using the pulse-amplitude modulation (PAM)

$$q(t,0) = \sum_{i=-\infty}^{+\infty} S_i p(t - iT),$$

where $p(t)$ is raised-cosine (RRC) pulse shape with bandwidth $B = 1/T$ and roll-off factor $r$. At the receiver, a neural equalizer and detector takes $q(t, L)$ and recovers the sequence of bits $\boldsymbol{m}$, denoted by $\widehat{\boldsymbol{m}}$.

The system was set based on 16-QAM transmission at 25 Gbaud using RRC pulses (roll-off factor 0.1), and with the fiber and noise parameters as follows: dispersion value $D$ of 17 $ps/(nm - km)$, nonlinearity parameter $\gamma$ of 1.27 $1/(W \cdot km)$, and noise PSD of $5.906 \times 10^{-21}$ $W/(km \cdot Hz)$.

## 4.2 NUMERICAL RESULTS

Equalization in the aforementioned system was considered using MLP, RNN, state-of-the-art (SOA) CNN [11], DBP, and chromatic dispersion compemsation (CDC). The details of the implantations are confidential at the moment of writing this document.

The BER performance of these approaches as a function of SNR, and simulation step size (for DBP), for a 500km, 1000km, and 2000km fiber-optic link, is illustrated in Fig. 4.1, Fig. 4.2, Fig.4.3, respectively.

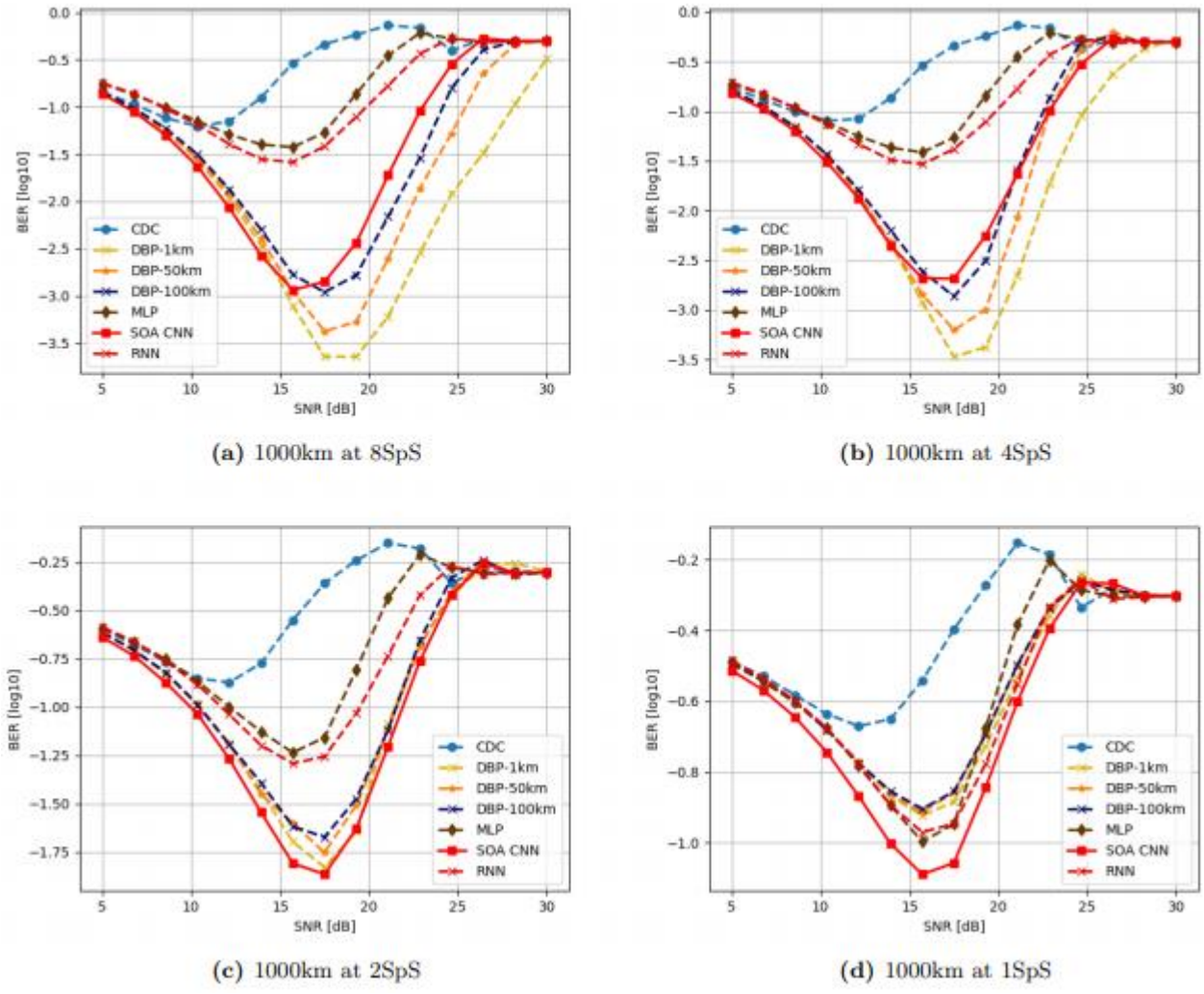


*Figure 4.2. The BER of the equalizers for the 1000km fiber-optic link, as a function of SNR for several values of sampling rates at RX and DBP step size.*

As a matter of fact, although CNNs are powerful in capturing short-temporal dependencies, they may not be efficient in capturing long-temporal features in terms of model size and complexity. In this regard, we contemplated and proposed a model capable of capturing long and short temporal features more efficiently in terms of performance complexity trade-off. This model achieves the same BER performance, at 1 and 2 samples/symbol, as the state-of-the-art CNN, while it has noticeably fewer model parameters and also lower memory and computational resource requirements for training. The details of this approach are confidential at the moment of writing this document.

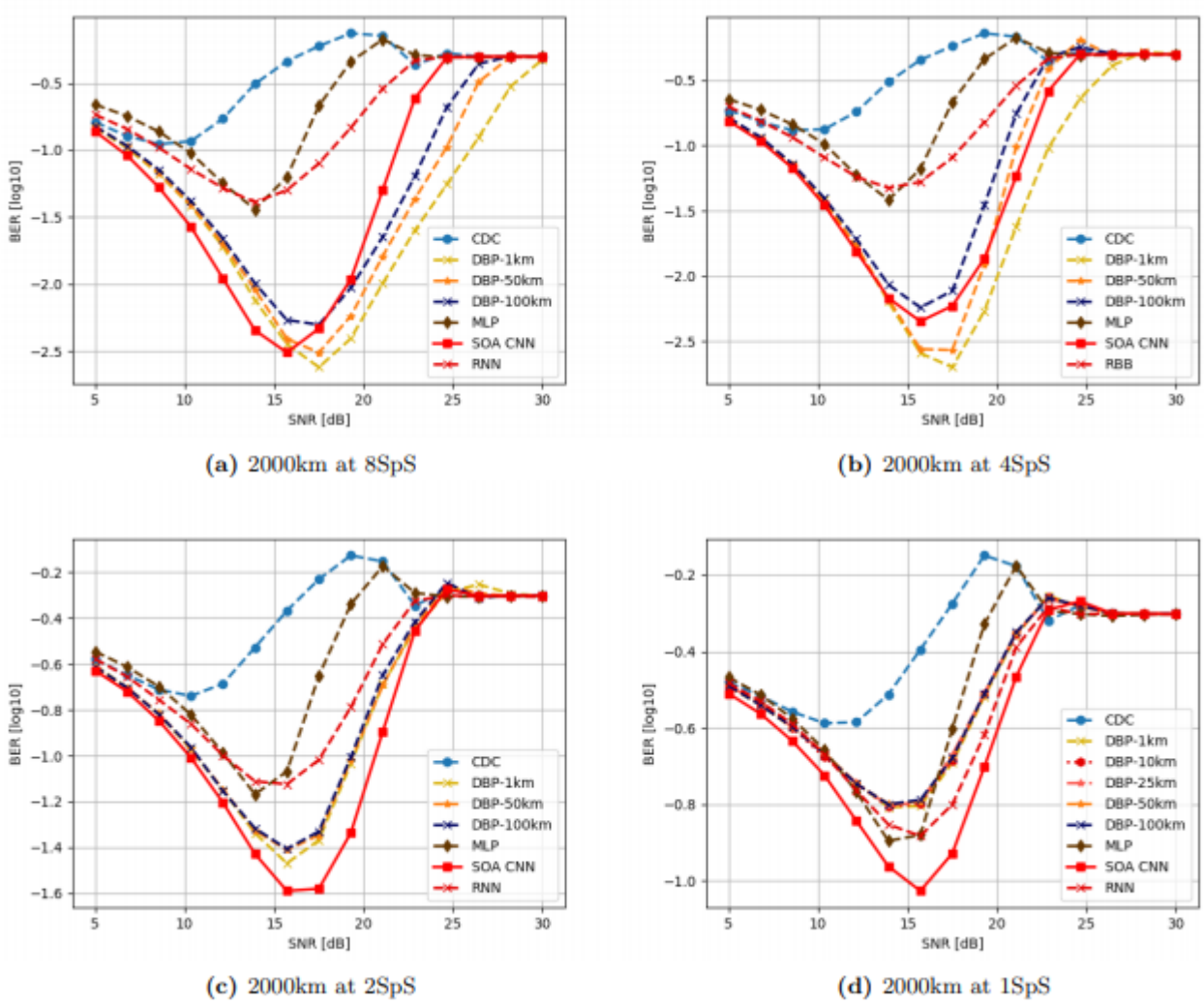


(a) 2000km at 8SpS (b) 2000km at 4SpS

(c) 2000km at 2SpS (d) 2000km at 1SpS

*Figure 4.3. The BER of the equalizers for the 2000km fiber-optic link, as a function of SNR for several values of sampling rates at RX and DBP step size.*

## 4.3 References (this section)

[1] Musumeci, Francesco, et al. "An overview on application of machine learning techniques in optical networks." IEEE Communications Surveys & Tutorials 21.2 (2018): 1383-1408.

[2] Catanese, Clara, et al. "A Survey of Neural Network Applications in Fiber Nonlinearity Mitigation." 2019 21st International Conference on Transparent Optical Networks (ICTON). IEEE, 2019.

[3] Catanese, Clara, et al. "A Fully Connected Neural Network Approach to Mitigate Fiber Nonlinear Effects in 200G DP-16-QAM Transmission System." 2020 22nd International Conference on Transparent Optical Networks (ICTON). IEEE, 2020.

[4] Kotlyar, Oleksandr, et al. "Combining nonlinear Fourier transform and neural network-based processing in optical communications." Optics Letters 45.13 (2020): 3462-3465.

[5] Karanov, Boris, et al. "End-to-end optimized transmission over dispersive intensity-modulated channels using bidirectional recurrent neural networks." Optics express 27.14 (2019): 19650-19663.

[6] Karanov, Boris, et al. "Optical fiber communication systems based on end-to-end deep learning." 2020 IEEE Photonics Conference (IPC). IEEE, 2020.

[7] Li, Peixuan, et al. "56 Gbps IM/DD PON based on 10G-class optical devices with 29 dB loss budget enabled by machine learning." 2018 Optical Fiber Communications Conference and Exposition (OFC). IEEE, 2018.

[8] Chuang, Chun-Yen, et al. "Convolutional neural network based nonlinear classifier for 112-Gbps high speed optical link." Optical Fiber Communication Conference. Optical Society of America, 2018.

[9] Butler, Rick M., et al. "Model-Based Machine Learning for Joint Digital Backpropagation and PMD Compensation." Journal of Lightwave Technology (2020).

[10] Häger, Christian, and Henry D. Pfister. "Nonlinear interference mitigation via deep neural networks." 2018 Optical Fiber Communications Conference and Exposition (OFC). IEEE, 2018.

[11] Häger, Christian, and Henry D. Pfister. "Deep learning of the nonlinear Schrödinger equation in fiber-optic communications." 2018 IEEE International Symposium on Information Theory (ISIT). IEEE, 2018.